PROCEEDINGS OF SCIENCE

Target space entanglement in the matrix model for bubbling geometry

Asato Tsuchiya[a,b,*] **and Kazushi Yamashiro**[b]

[a] *Department of Physics, Shizuoka University, 836 Ohya, Suruga-ku, Shizuoka 422-8529, Japan*

[b] *Graduate School of Science and Technology, Shizuoka University 836 Ohya, Suruga-ku, Shizuoka 422-8529, Japan*

E-mail: tsuchiya.asato@shizuoka.ac.jp, yamashiro.kazushi.17@shizuoka.ac.jp

We study the target space entanglement entropy in the context of the bubbling AdS geometry. We consider it in a complex matrix model which describes the chiral primary sector in $\mathcal{N} = 4$ super Yang-Mills theory. The targe space in this case is a two-dimensional plane where the eigenvalues of the complex matrix distribute. It is identified with a plane in the bubbling geometry where the boundary condition is fixed by specifying a droplet that is identified with the eigenvalue distribution. We calculate the target space entanglement entropy of a subregion in the plane for each of states in the matrix model that correspond to $AdS_5 \times S^5$, an AdS giant graviton and a giant graviton in the bubbling geometry. We find that it agrees qualitatively with the area of the boundary of the subregion in the bubbling geometry

Corfu Summer Institute 2021 "School and Workshops on Elementary Particle Physics and Gravity"
29 August - 9 October 2021
Corfu, Greece

*Speaker

PoS(CORFU2021)256

1. Introduction

Much attention has been paid to quantum entanglement in construction of quantum gravity, since it seems to be deeply connected to emergent geometry[1]. Recently, a new type of quantum entanglement called the target space entanglement entropy has been investigated in the context of the gauge/gravity correspondence[2–9]. While the ordinary entanglement entropy is defined by dividing the base space of field theory, target space entanglement entropy is defined by dividing the configuration space of fields. In particular, the latter can be defined even in $(0+1)$-dimensional field theory, namely quantum mechanics, although the latter cannot.

For instance, in matrix quantum mechanics, a space where the eigenvalues of the matrix distribute can be viewed as a target space. It seems difficult to define entanglement entropy in gravitational theories, since division of dynamical spaces is nontrivial. The authors of [3] have conjectured in the gauge/gravity correspondence that the entanglement entropy in the bulk can be defined by the target space entanglement entropy on the gauge theory side. In particular, the target space entanglement entropy of a subregion in the D0-brane quantum mechanics[10] is expected to be proportional with factor of proportionality $1/4G_N$ to the area of boundary of the corresponding subregion in the bulk on the gravity side.

This talk is based on [8]. We consider the target space entanglement entropy in the D3-brane holography, namely a conjectured correspondence between $\mathcal{N}=4$ super Yang-Mills theory (SYM) and type IIB superstring theory on $AdS_5\times S^5$[11–13]. Here we focus on a correspondence between the chiral primary sector of $\mathcal{N}=4$ SYM and the bubbling AdS geometry[14–16]. The former can be described by a complex matrix model[17]. The target space in this case is a two-dimensional plane where the eigenvalues of the complex matrix distribute (see also [18]). The target space can be identified with a two-dimensional plane in the bubbling geometry where a boundary condition for a half-BPS solution with $R\times SO(4)\times SO(4)$ symmetry in type IIB supergravity is specified by giving a droplet that is identified with the eigenvalue distribution. We calculate the target space entanglement entropy of a subregion in the two-dimensional plane for each of states that correspond to $AdS\times S^5$, an AdS giant graviton and a giant graviton and compare it with the area (length) of boundary of the corresponding subregion in the bubbling geometry. We find a qualitative agreement between the target space entanglement entropy and the area.

2. Review

In this section, we review some materials in brief.

2.1 Complex matrix model and fermions in two-dimensional plane

The chiral primary operators in $\mathcal{N}=4$ SYM, which are hal-BPS holomorphic operators, take the form

$$O^{J_1,J_2,\cdots,J_K}(t)=\prod_{a=1}^{K}\mathrm{Tr}(Z^{J_a})\ , \tag{1}$$

where $Z=\frac{1}{\sqrt{2}}(\phi_1+i\phi_2)$ with ϕ_1 and ϕ_2 being two of six scalars. Kaluza-Klein gravitons and (AdS) giant gravitons on the gravity side are represented in terms of a linear combination of the operators

(1). The dynamics of the operators is described by a complex matrix model which is obtained by dimensionally reducing the free part of the action for Z on $R \times S^3$ to R [17]. The complex matrix model is defined by

$$\mathcal{Z} = \int [dZ(t)dZ^\dagger(t)]e^{iS} \,,$$
$$S = \int dt \mathrm{Tr}(\dot{Z}(t)\dot{Z}^\dagger(t) - Z(t)Z^\dagger(t)) \,, \tag{2}$$

where $Z(t)$ is an $N \times N$ complex matrix depending on the time, and the path integral measure is defined by a norm in matrix configuration space,

$$||dZ(t)||^2 = 2\mathrm{Tr}(dZ(t)dZ^\dagger(t)) \tag{3}$$

The hamiltonian is given by

$$\hat{H} = \sum_{i,j}\left(-\frac{\partial}{\partial Z_{ij}\partial Z^*_{ij}} + Z_{ij}Z^*_{ij}\right) \,. \tag{4}$$

The wave function of the ground state is given by

$$\chi_0 = \frac{1}{\pi^{\frac{N^2}{2}}}e^{-\mathrm{Tr}(ZZ^\dagger)} = \frac{1}{\pi^{\frac{N^2}{2}}}e^{\Sigma_{i,j}Z_{ij}Z^*_{ij}} \,, \tag{5}$$

and the wave functions of excited states that correspond to the chiral primary states are given by

$$\chi^{(J_1,\cdots,J_K)} = \left(\prod_{a=1}^{K}\mathrm{Tr}(Z^{J_a})\right)\chi_0 \,. \tag{6}$$

The complex matrix Z is decomposed as $Z = UTU^\dagger$ in terms of a unitary matrix U and an upper triangular matrix T. The eigenvalues of Z are given by $z_i = T_{ii}$ $(i = 1, \cdots, N)$. The wave functions (6) are rewritten in terms of z_i and T_{ij} $(i < j)$ as

$$\chi^{(J_1,\cdots,J_K)} = \left(\prod_{a=1}^{K}\sum_{i_a} z_{i_a}^{J_a}\right)\chi_0 \,,$$
$$\chi_0 = \frac{1}{\pi^{\frac{N^2}{2}}}e^{-\Sigma_i z_i z_i^* - \Sigma_{j<k}T_{jk}T^*_{jk}} \,, \tag{7}$$

while the path integral measure as

$$\int\prod_{i,j}dZ_{ij}dZ^*_{ij} = \int\prod_{i>j}dH_{ij}dH^*_{ij}\prod_{k<l}dT_{kl}dT^*_{kl}\prod_{m}dz_m dz^*_m|\Delta(z)|^2 \,, \tag{8}$$

where $\Delta(z) = \prod_{i<j}(z_i - z_j)$ and $dH = -iU^\dagger dU$. We can absorb $\Delta(z)$ into the wave function and define a new wave function χ_F by $\chi_F \equiv \Delta(z)\chi$. Then, χ_F is represented as a certain linear combination of

$$\frac{1}{\sqrt{N!}}\det(\Phi_{l_i}(z_j, z_j^*)) \times \prod_{j<k}\Phi_0(T_{jk}, T^*_{jk}) \,,$$
$$\text{with} \quad \sum_i l_i = \frac{N(N-1)}{2} + \sum_{a=1}^{K} J_a \,, \tag{9}$$

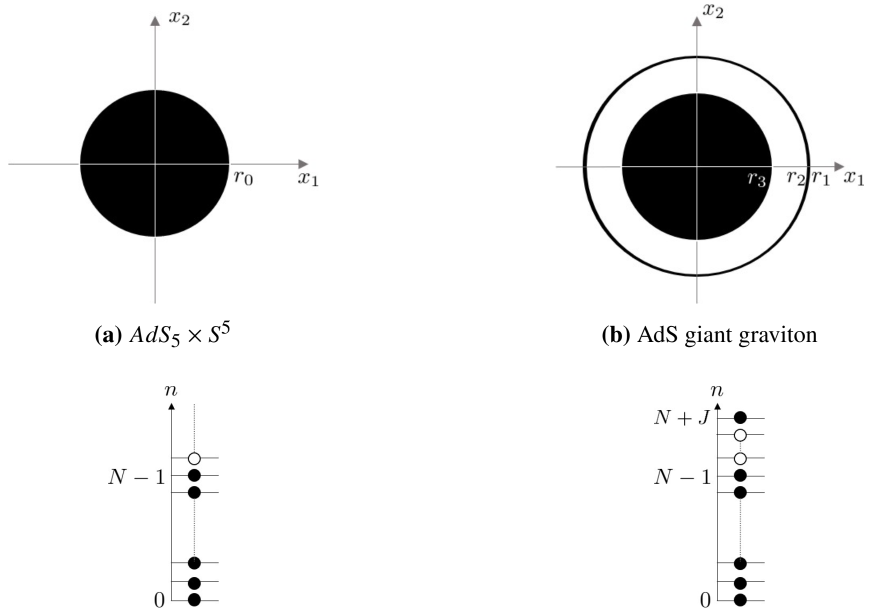

(a) $AdS_5 \times S^5$ **(b)** AdS giant graviton

(c) $AdS_5 \times S^5$ **(d)** AdS giant graviton

Figure 1: (1a) and (1b) are droplets of the states that correspond to $AdS_5 \times S^5$ and an AdS giant graviton, respectively. (1c) and (1d) are the occupied energy levels of the states that correspond to $AdS_5 \times S^5$, an AdS giant graviton, respectively.

where $\Phi_l(z, z^*)$ are the wave function of the lowest Landau level which takes the form

$$\Phi_l(z, z^*) = \sqrt{\frac{2^l}{l!\pi}} z^l e^{-zz^*} , \tag{10}$$

and can be viewed as a wave function of the holomorphic sector for a particle in the harmonic oscillator potential in two-dimensional plane. (9) is a wave function for N fermions and $\frac{1}{2}N(N-1)$ bosons in the harmonic oscillator potential. The eigenvalues z_i of Z can be viewed as the coordinates of N fermions, while (T_{ij}, T_{ij}^*) as those of $\frac{1}{2}N(N-1)$ bosons. Since the bosons are always in the ground state, we can integrate out T_{ij} and concentrate on $\frac{1}{\sqrt{N!}}\det(\Phi_{l_i}(z_j, z_j^*))$ in (9). In this way, we can reduce the holomorphic sector of the complex matrix model, which describes the dynamics of the operators (1), to a system of N fermions in the two-dimensional harmonic oscillator potential. For large N, we can view the eigenvalue distribution corresponding to a state as a droplet in the complex plane, which is formed by N fermions.

In what follows, we focus on two particular states whose wave functions are given by

$$\frac{1}{\sqrt{N!}}\det(\Phi_{l_i}(z_j, z_j^*)) \tag{11}$$

in (9). The first one is the ground state where $l_1 = 0,\ l_2 = 1,\ \cdots,\ l_N = N-1$. We show the corresponding droplet in Fig. 1a and the occupied energy levels in Fig. 1c. This corresponds to $AdS_5 \times S^5$ in the bubbling geometry. The second one is an excited state where $l_1 = 0,\ l_2 = 1,\ \cdots,\ l_N = N-1,\ l_{N+1} = N+J$. Note that the total number of fermions is $N+1$. We show the corresponding droplet in Fig. 1b and the occupied energy levels in Fig. 1d. This corresponds to a bubbling geometry where there exists an AdS giant graviton, which is a D3-brane wrapped on S^3 in AdS_5. As for an excited state corresponding to a bubbling geometry where there exists a giant graviton, which is a D3-brane wrapped on S^3 in S^5, see [8]. The wave function $\Phi_l(z, z^*)$ is localized on a circle centered at the origin with the radius $\sqrt{l}$. Hence, r_0 in Fig. 1a is equal to $\sqrt{N}$ for large N.

2.2 Bubbling geometry

Next, we review the bubbling geometry which was developed by Lin, Lunin and Maldacena. They gave the general form of half-BPS solutions with $R \times SO(4) \times SO(4)$ symmetry in type IIB supergravity [16]. The metric takes the form

$$ds^2 = -h^{-2}\left[dt + \sum_{i=1}^{2} V_i dx^i\right]^2 + h^2\left[dy^2 + \sum_{i=1}^{2} dx^i dx^i\right] + ye^G d\Omega_3^2 + ye^{-G} d\tilde{\Omega}_3^2 , \qquad (12)$$

where

$$h^{-2} = 2y\cosh G, \quad z = \frac{1}{2}\tanh G, \quad y\partial_y V_i = \epsilon_{ij}\partial_j z, \quad y(\partial_i V_j - \partial_j V_i) = \epsilon_{ij}\partial_y z . \qquad (13)$$

The solutions are completely determined by the function $z(x_1, x_2, y)$, which obeys a differential equation

$$\partial_i\partial_i z + y\partial_y\left(\frac{\partial_y z}{y}\right) = 0 . \qquad (14)$$

The function z is fixed by specifying a boundary condition at $y = 0$, and z must take $1/2$ or $-1/2$ at $y = 0$. 'black' is assigned to the region with $z = -1/2$, while 'white' to the region with $z = 1/2$. Thus, there is a correspondence between divisions of the $x_1 - x_2$ plane into black and white regions and half-BPS solutions with $R \times SO(4) \times SO(4)$ symmetry. The two-dimensional plane specified by $y = 0$ in the bubbling geometry can identified with the target space in the complex matrix model such that black regions correspond to droplets in the target space. Figs 1a and 1b correspond to $AdS_5 \times S^5$, an AdS giant graviton, respectively, as mentioned before. Here r_0 in Fig.1a is related to the radius of AdS_5 as $r_0 = R_{AdS}^2 = \sqrt{N}$.

2.3 Target Space Entanglement Entropy

Finally, we review the target space entanglement entropy[2]. As a concrete example, we consider a quantum mechanics of N identical particles in d dimensions. In this case, the target space is the d-dimensional space where N particle live. Division of the target space into a subregion A and its complement $\bar{A}$ leads to decomposition of the total Hilbert space $\mathcal{H}$ as

$$\mathcal{H} = \bigoplus_n \mathcal{H}_{A,n} \otimes \mathcal{H}_{\bar{A},n} , \qquad (15)$$

where n labels a sector where n particles exist in A and $N - n$ particles exist in $\bar{A}$. The target space entanglement entropy of the subregion A is given by

$$S_A = -\sum_n p_n \log p_n + \sum_n p_n S_{A,n} , \qquad (16)$$

where p_n is the probability of realization of the sector n, which is given by

$$p_n = \binom{N}{n} \int_A \prod_{a=1}^{n} d^d x_a \int_{\bar{A}} \prod_{b=n+1}^{N} d^d y_b |\psi(\vec{x}_1, \cdots, \vec{x}_n, \vec{y}_{n+1}, \cdots, \vec{y}_N)|^2 . \tag{17}$$

The first and second terms in the RHS of (16) is classical and quantum parts, respectively. $S_{A,n}$ is interpreted as the entanglement entropy of the subregion A in the sector n, which is given by

$$S_{A,n} = -\mathrm{tr}_{A,n} \rho_{A,n} \log \rho_{A,n} , \tag{18}$$

where $\rho_{A,n}$ is the reduced density matrix of the sector n and its matrix elements in the coordinate basis are given by

$$\langle \vec{x} | \rho_{A,n} | \vec{x}' \rangle = \frac{1}{p_n} \binom{N}{n} \int_{\bar{A}} \prod_{b=n+1}^{N} d^d y_b \psi(\vec{x}, \vec{y}) \psi^*(\vec{x}', \vec{y}) . \tag{19}$$

In the following, we focus on the case of N identical fermions which are not interacting each other[6]. The wave function is given by a Slater determinant

$$\psi(\vec{x}_1, \cdots \vec{x}_N) = \frac{1}{\sqrt{N!}} \det(\chi_i(\vec{x}_j)) , \tag{20}$$

where $\chi_i(\vec{x})$ are orthonormal single-body wave functions:

$$\int d^d x \chi_i^*(\vec{x}) \chi_j(\vec{x}) = \delta_{ij} . \tag{21}$$

We introduce an $N \times N$ overlap matrix X_{ij}

$$X_{ij} \equiv \int_A d^d x \, \chi_i(\vec{x}) \chi_j^*(\vec{x}) , \tag{22}$$

Because X_{ij} is a hermitian matrix, it can be diagonalized by a unitary matrix U_{ij}. The eigenvalues of X_{ij} denoted by λ_i are given by

$$\lambda_i = \int_A |\tilde{\chi}_i(\vec{x})^2| , \tag{23}$$

where $\tilde{\chi}_i(\vec{x}) = U_{ij} \chi_j(\vec{x})$. λ_i is the probability of existence in the region A when the wave function for a particle is given by $\tilde{\chi}_i(\vec{x})$.

p_n in (17) is given by

$$p_n = \sum_{I \in F_n} \prod_{i \in I} \lambda_i \prod_{j \in \bar{I}} (1 - \lambda_j) . \tag{24}$$

Here F_n is a set of all subsets of $\{1, \ldots, N\}$ that consist of n elements. p_n is indeed the probability that n particles exist in the region A when the probability that each of N particles exists in A is given by λ_i.

The matrix elements of $\rho_{A,n}$ in (19) are

$$\langle \vec{x} | \rho_{A,n} | \vec{x}' \rangle = \frac{1}{p_n} \sum_{I \in F_n} \lambda_I \bar{\lambda}_I \psi_I(\vec{x}) \psi_I^*(\vec{x}') , \tag{25}$$

where we put $\lambda_I \equiv \prod_{i\in I}\lambda_i$ and $\bar\lambda_I \equiv \prod_{i\in I}(1-\lambda_i)$ for an element I of F_n and introduce a wave function for n particles

$$\psi_I = \frac{1}{\sqrt{\lambda_I}}\sum_{\sigma\in S_n}\frac{(-1)^\sigma}{\sqrt{n!}}\tilde\chi_{n_{\sigma(1)}}(\vec{x}_1)\cdots\tilde\chi_{n_{\sigma(n)}}(\vec{x}_n)\ . \tag{26}$$

The quantum part is calculated as

$$\sum_{n=0}^{N} p_n S_{A,n} = \sum_{n=0}^{N} p_n\log p_n - \sum_{n=0}^{N}\sum_{I\in F_n}\lambda_I\bar\lambda_I\log(\lambda_I\bar\lambda_I)\ . \tag{27}$$

Thus, we see from (25) and (27) that the total target space entanglement entropy (16) is given by

$$S_A = -\sum_{n=0}^{N}\sum_{I\in F_n}\lambda_I\bar\lambda_I\log(\lambda_I\bar\lambda_I). \tag{28}$$

By introducing $H(\lambda)\equiv -\lambda\log\lambda-(1-\lambda)\log(1-\lambda)$, we represent (28) as[1]

$$S_A = \sum_{i=1}^{N} H(\lambda_i)\ , \tag{29}$$

where $H(\lambda)$ is the Shannon entropy for the Bernoulli distribution $(\lambda, 1-\lambda)$.

3. Target Space Entanglement Entropy in the complex matrix model

In this section, we calculate the target space entanglement entropy for the two states in the complex matrix model introduced in section 2.1. We consider a circle centered at the origin with the radius r as a subregion A. Then, the overlap matrix (22) is given by

$$\begin{aligned} X_{ll'}(A) &= 2\int_A dzdz^*\Phi_l(z,z^*)\Phi_{l'}(z,z^*) \\ &= \delta_{ll'}a_l(r)\ . \end{aligned} \tag{30}$$

The eigenvalues λ_l are

$$\lambda_l = a_l(r) = \frac{\gamma[l+1,r^2]}{\Gamma[l+1]}\ , \tag{31}$$

where $\Gamma[x]$ is the gamma function and $\gamma[a,x]$ is the incomplete gamma function:

$$\gamma[a,x] = \int_0^x t^{a-1}e^{-t}dt\ . \tag{32}$$

[1]This formula was obtained in [19–21] in the context of condensed matter and statistical physics.

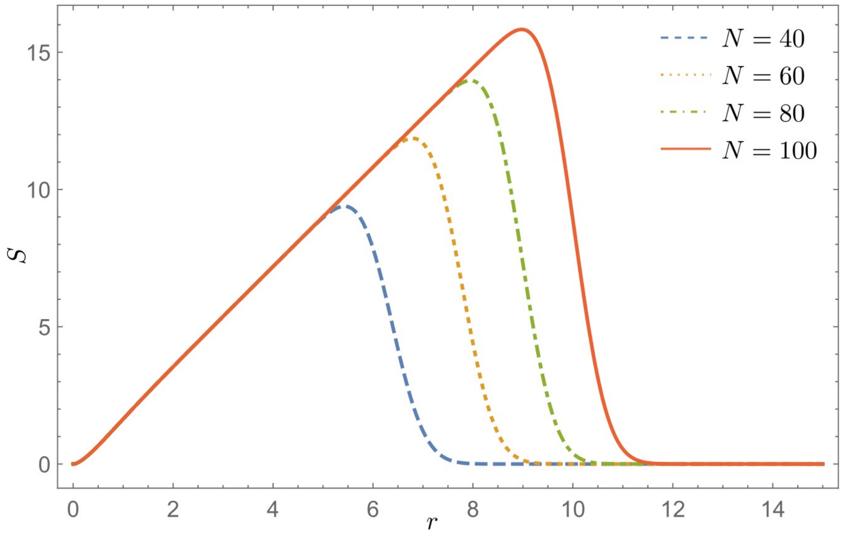

Figure 2: The target space entanglement entropy for the ground state S_0 with $N = 40,\ 60,\ 80,\ 100$ are plotted against the radius r of the subregion A.

λ_l is the provability of existence in A of a single particle. By using (28)[2], we evaluate the target space entanglement entropy of the subregion A. The result is

$$S(r,N) = \sum_{i=1}^{N} H(a_{l_{(i)}}(r)), \quad H(a_{l_{(i)}}(r)) = -a_{l_{(i)}}(r) \log a_{l_{(i)}}(r) - (1 - a_{l_{(i)}}(r)) \log(1 - a_{l_{(i)}}(r)) \ . \tag{33}$$

First, let us calculate the target space entanglement entropy for the ground state indicated in Figs. 1a and 1c, which correspond to $AdS_5 \times S^5$ in the bubbling geometry. (33) in this case is

$$S_0(r,N) = \sum_{l=0}^{N-1} H(a_l(r)), \ H(a_l(r)) = -a_l(r) \log a_l(r) - (1 - a_l(r)) \log(1 - a_l(r)) \ . \tag{34}$$

In Fig. 2, the target space entanglement entropy S_0 for $N = 40,\ 60,\ 80,\ 100$ is plotted against r. We see that S_0 is proportional to r as $S_0 = 1.81r$ when the subregion A is included in the droplet, namely $r < \sqrt{N}$. This behavior shows that the entanglement entropy is proportional to the area of boundary of the subregion A. The fact that $S_0 = 0$ when the droplet is included in the subregion A, namely $r > \sqrt{N}$, shows that there is no entanglement between inside and outside of A because all particles are confined in A. This is a finite N effect[3] .

Second, we calculate the target space entanglement entropy for an excited state corresponding to an AdS giant graviton indicated in Figs. 1b and 1d. (33) in this case is

$$S_{AdS}(r,N,J) = \sum_{i=0}^{N-1} H(a_i(r)) + H(a_{N+J}(r)) \ . \tag{35}$$

In Fig. 3, S_{AdS} for $N = 50$ and $J = 50$ is plotted against r. In order to see only the contribution of

[2]Here we simply consider the full Hilbert space for N fermions in two-dimensional plane in calculating the reduced density matrix.

[3]In [20], S_0 was calculated in the $N \to \infty$ limit. The result is that $S_0 = 2\sqrt{2\pi} r \int_{-\infty}^{\infty} \frac{d\mu}{2\pi} H(\frac{1}{2}\mathrm{Erfc}(\mu)) \sim 1.804r$ for

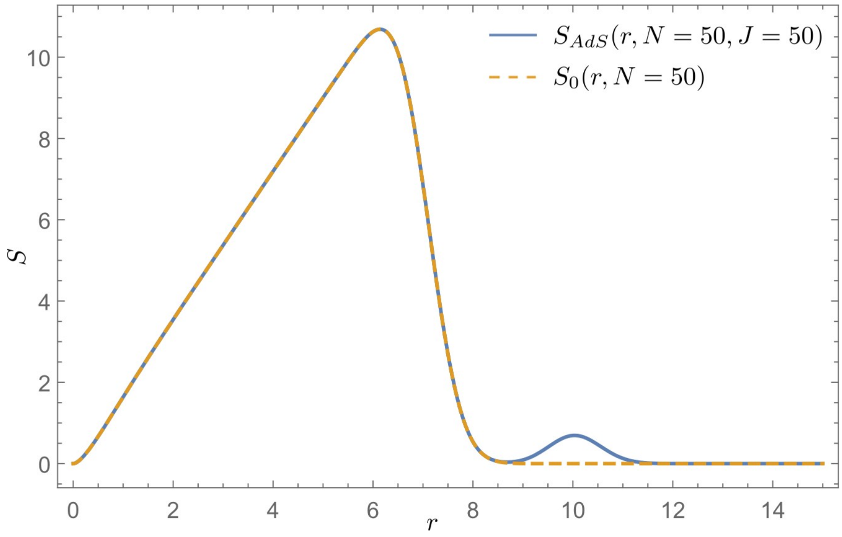

Figure 3: The solid line represents the target space entanglement entropy for the state corresponding to the AdS giant graviton $S_{AdS}(r)$ with $N = 50$ and $J = 50$, while the dashed line represents the target space entanglement entropy for the ground state $S_0(r)$ with $N = 50$.

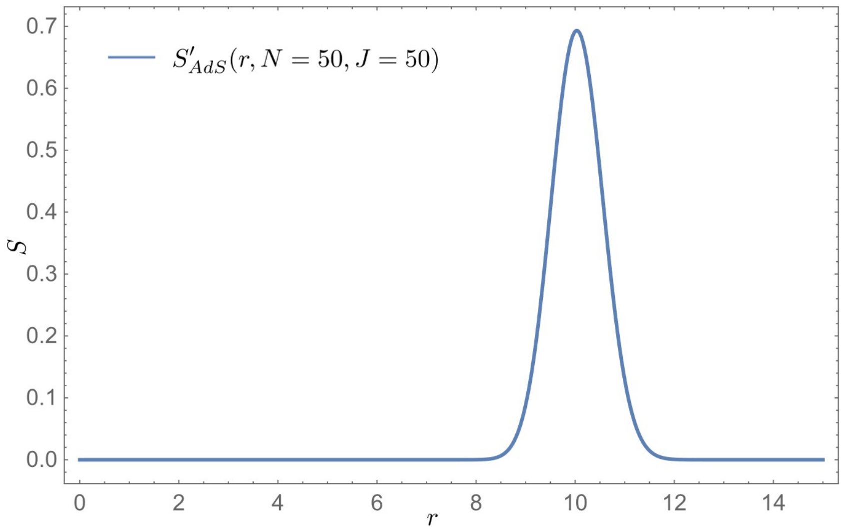

Figure 4: $S'_{AdS} = S_{AdS}(r, 50, 50) - S_0(r, 50)$ is plotted against r.

the AdS giant graviton to the target space entanglement entropy, we subtract S_0 from S_{AdS}. In Fig. 4, $S'_{AdS} = S_{AdS}(r, 50, 50) - S_0(r, 50)$ is plotted against r. Note here that N for S_{AdS} is different from that for S_0. We see that there is a peak at $r = \sqrt{N + 1 + J}$, which is considered as the position of the AdS giant graviton.

As for the target space entanglement entropy for an excited state corresponding to a giant graviton, see [8].

$0 \leq r < \infty$.

4. Area of boundary in the bubbling AdS geometry

In this section, we calculate the area (length) of boundary of the subregion A in the bubbling geometry.

We introduce the polar coordinates $(\tilde{r}, \phi)$ in the $x_1 - x_2$ plane. The solution determined by a droplet in Fig. 1a corresponding to $AdS_5 \times S^5$ is given by [16]

$$\tilde{z}(\tilde{r}, y; r_0) \equiv z - \frac{1}{2} = \frac{\tilde{r}^2 - r_0^2 + y^2}{2\sqrt{(\tilde{r}^2 + r_0^2 + y^2)^2 - 4\tilde{r}^2 r_0^2}} - \frac{1}{2} ,$$
$$V_\phi = -\frac{1}{2}\left(\frac{\tilde{r}^2 + r_0^2 + y^2}{\sqrt{(\tilde{r}^2 + r_0^2 + y^2)^2 - 4\tilde{r}^2 r_0^2}} - 1 \right) , \tag{36}$$

where r_0 is related to the radius of AdS_5 as $r_0 = R_{AdS}^2 = \sqrt{N}$.

Using (36), a solution for a general circular symmetric droplet can be constructed as [16]

$$\tilde{z} = \sum_i (-1)^{i+1} \tilde{z}(\tilde{r}, y; r_i), \; V_\Phi = \sum_i (-1)^{i+1} V_\phi(\tilde{r}, y; r_i) , \tag{37}$$

where r_1 is the radius of the most outer circle and r_2 is the radius of the second outer circle and so on. We can construct z corresponding to the droplets in Fig. 1b using (37).

We identify the target space of the complex matrix model with the $x_1 - x_2$ plane at $y = 0$ and consider the subregion A in the $x_1 - x_2$ plane. We calculate the area (length) of boundary of A using the metric (12). The induced metric in the $x_1 - x_2$ plane at $y = 0$ denoted by γ_{ij} is

$$\gamma_{\tilde{r}\tilde{r}} = h^2, \; \gamma_{\phi\phi} = -h^{-2} V_\phi^2 + h^2 \tilde{r}^2, \; \gamma_{\tilde{r}\phi} = \gamma_{\phi\tilde{r}} = 0 . \tag{38}$$

Then , the area (length) of the boundary of A in the $x_1 - x_2$ plane, which we denote by L, is given by

$$L(r) = \int_0^{2\pi} d\phi \sqrt{\gamma_{\phi\phi}} = 2\pi \sqrt{-h^{-2} V_\phi^2 + h^2 r^2} , \tag{39}$$

where h and V_ϕ are defined in (13).

First of all, we calculate the area of boundary of A for $AdS_5 \times S^5$. We see from (36) that $\gamma_{\phi\phi}$ is in the $y \to 0$ limit given by

$$\gamma_{\phi\phi} = \lim_{y \to 0} (-h^{-2} V_\phi^2 + h^2 \tilde{r}^2) = \frac{\tilde{r}^2 + r_0^2 - |\tilde{r}^2 - r_0^2|}{2r_0} . \tag{40}$$

Thus, the length of the boundary of A is

$$L(r) = \int_0^{2\pi} \sqrt{\gamma_{\phi\phi}} = \sqrt{2}\pi \sqrt{\frac{r^2 + r_0^2 - |r^2 - r_0^2|}{r_0}} . \tag{41}$$

L is proportional to r for $r < r_0$: $L(r) = \sqrt{\frac{2}{r_0}}\pi r$. This behavior qualitatively agrees with that of the target space entanglement entropy in Fig. 2. L is constant for $r > r_0$,: $L(r) = \sqrt{2r_0}\pi$. As for the calculation of the area of the boundary of A for an AdS giant graviton and a giant graviton, see [8].

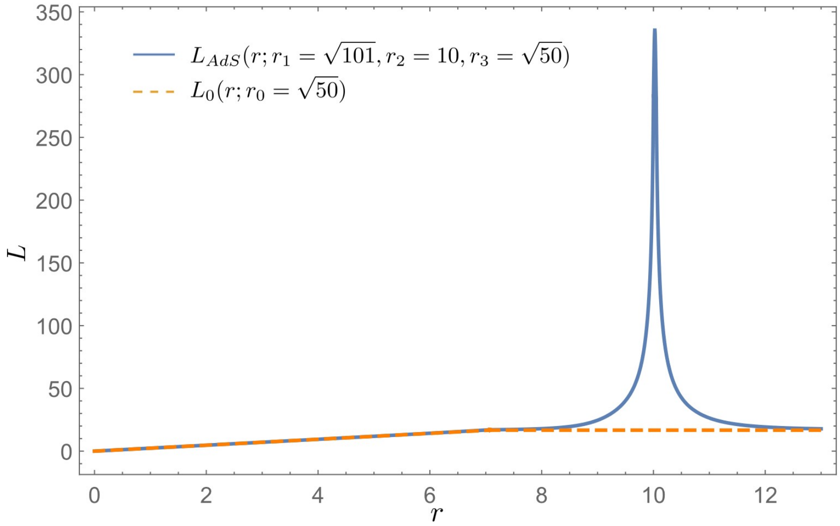

Figure 5: The solid line represents the area of the boundary of the subregion A for an AdS giant graviton L_{AdS} with $r_1 = \sqrt{101}, r_2 = 10$ and $r_3 = \sqrt{50}$, while the dashed line represents that for the ground state L_0 with $r_0 = \sqrt{50}$.

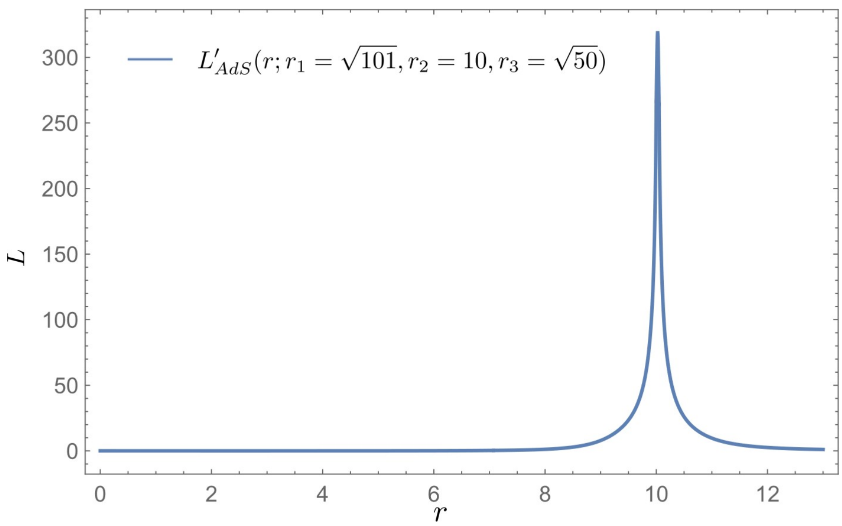

Figure 6: $L'_{AdS} = L_{AdS}(r) - L_0(r)$ is plotted against r.

We denote the area of boundary of A for $AdS_5 \times S^5$ and an AdS giant graviton by $L_0(r)$. $L_{AdS}(r)$, respectively. In Fig. 5, $L_{AdS}(r)$ for $r_1 = \sqrt{101}, r_2 = 10, r_3 = \sqrt{50}$ and $L_0(r)$ for $r_0 = r_3$ are plotted against r. As in the target space entanglement entropy, we subtract L_0 from L_{AdS}. In Fig .6, $L'_{AdS} = L_{AdS}(r) - L_0(r)$ is plotted against r. We see that L'_{AdS} has a peak around $r = r_1 = \sqrt{N}$. This behavior of L'_{AdS} qualitatively agrees with S'_{AdS} in Fig. 4.

In this way, we find that the contribution of an AdS giant graviton to the area (length) of boundary of A qualitatively agrees with that to the target space entanglement entropy. We have also seen the similar qualitative agreement for a giant graviton[8].

5. Conclusion and discussion

In this talk, we studied the target space entanglement entropy in the complex matrix mode that describes the chiral primary sector of $\mathcal{N} = 4$ SYM on $R \times S^3$, which is associated with the bubbling AdS geometry. The target space of the complex matrix model is a two-dimensional plane where the eigenvalues of the complex matrix distribute and form droplets. This two-dimensional plane is identified with that in the bubbling geometry, where the boundary conditions for the solutions are specified by the droplets. We calculated the target space entanglement entropy of a subregion in two-dimensional plane with droplets corresponding to $AdS_5 \times S^5$, an AdS giant graviton and a giant graviton in the bubbling geometry. We also calculated the area of boundary of the subregion in the bubbling geometry, and found a qualitative agreement between the target space entanglement entropy and the area of boundary.

In order to see whether the target space entanglement entropy and the area agree quantitatively, we need to evaluate the effective Newton constant in (2+1)-dimensional space-time consisting of the two-dimensional plane and the time and fix the factor of proportionality $1/4G_N$ between the target space entanglement entropy and the area. Possibly, more elaborated correspondence between chiral primary states and droplets is needed. We hope to report progress in these issues in the near future.

Acknowledgments

A.T. would like to thank the organizers of Corfu 2021. A.T. was supported in part by Grant-in-Aid for Scientific Research (No. 18K03614 and No. 21K03532) from Japan Society for the Promotion of Science. K.Y. was supported in part by Grant-in-Aid for JSPS Fellows (No. 20J13836).

References

[1] S. Ryu and T. Takayanagi, Phys. Rev. Lett. **96**, 181602 (2006) [arXiv:hep-th/0603001 [hep-th]].

[2] E. A. Mazenc and D. Ranard, [arXiv:1910.07449 [hep-th]].

[3] S. R. Das, A. Kaushal, G. Mandal and S. P. Trivedi, J. Phys. A **53**, no.44, 444002 (2020) [arXiv:2004.00613 [hep-th]].

[4] S. R. Das, A. Kaushal, S. Liu, G. Mandal and S. P. Trivedi, JHEP **04**, 225 (2021) [arXiv:2011.13857 [hep-th]].

[5] H. R. Hampapura, J. Harper and A. Lawrence, JHEP **10**, 231 (2021) [arXiv:2012.15683 [hep-th]].

[6] S. Sugishita, JHEP **08**, 046 (2021) [arXiv:2105.13726 [hep-th]].

[7] A. Frenkel and S. A. Hartnoll, [arXiv:2111.05967 [hep-th]].

[8] A. Tsuchiya and K. Yamashiro, JHEP **04**, 086 (2022) [arXiv:2201.06871 [hep-th]].

[9] S. R. Das, S. Hampton and S. Liu, [arXiv:2201.08330 [hep-th]].

[10] T. Banks, W. Fischler, S. H. Shenker and L. Susskind, Phys. Rev. D **55**, 5112-5128 (1997) [arXiv:hep-th/9610043 [hep-th]].

[11] J. M. Maldacena, Adv. Theor. Math. Phys. **2**, 231-252 (1998) [arXiv:hep-th/9711200 [hep-th]].

[12] S. S. Gubser, I. R. Klebanov and A. M. Polyakov, Phys. Lett. B **428**, 105 (1998) [hep-th/9802109].

[13] E. Witten, Adv. Theor. Math. Phys. **2**, 253 (1998) [hep-th/9802150].

[14] S. Corley, A. Jevicki and S. Ramgoolam, Adv. Theor. Math. Phys. **5**, 809-839 (2002) [arXiv:hep-th/0111222 [hep-th]].

[15] D. Berenstein, JHEP **07**, 018 (2004) [arXiv:hep-th/0403110 [hep-th]].

[16] H. Lin, O. Lunin and J. M. Maldacena, JHEP **10**, 025 (2004) [arXiv:hep-th/0409174 [hep-th]].

[17] Y. Takayama and A. Tsuchiya, JHEP **10**, 004 (2005) [arXiv:hep-th/0507070 [hep-th]].

[18] A. Ghodsi, A. E. Mosaffa, O. Saremi and M. M. Sheikh-Jabbari, Nucl. Phys. B **729**, 467-491 (2005) [arXiv:hep-th/0505129 [hep-th]].

[19] I. Klich, J. Phys. A **39**, L85-L92 (2006) [arXiv:quant-ph/0406068 [quant-ph]].

[20] I. D. Rodriguez and G. Sierra, Phys. Rev. B **80**, 153303 (2009) [arXiv:0811.2188 [cond-mat.mes-hall]].

[21] P. Calabrese, M. Mintchev and E. Vicari, Phys. Rev. Lett. **107**, 020601 (2011) [arXiv:1105.4756 [cond-mat.stat-mech]].

PoS(CORFU2021)256